Nanomolar detection of the antitumor drug tamoxifen by flexible organic electrochemical devices

Nanomolar detection of the antitumor drug tamoxifen by flexible organic electrochemical devices

P. D'Angelo, G. Tarabella, A. Romeo, S. L. Marasso, M. Cocuzza, C. Peruzzi, D. Vurro, G. Carotenuto, and S. Iannotta

Citation: AIP Conference Proceedings **1990**, 020015 (2018); doi: 10.1063/1.5047769
View online: https://doi.org/10.1063/1.5047769
View Table of Contents: http://aip.scitation.org/toc/apc/1990/1
Published by the American Institute of Physics

Nanomolar Detection of the Antitumor Drug Tamoxifen by Flexible Organic Electrochemical Devices

P. D'Angelo[1], G. Tarabella[1,2], A. Romeo[1,3], S. L. Marasso[1, 4], M. Cocuzza[1, 4], C. Peruzzi[1], D. Vurro[1], G. Carotenuto[5] and S. Iannotta[1,a)]

[1] *IMEM-CNR, Institute of Materials for Electronics and Magnetism, P.co Area delle Scienze 37/A, 43124, Parma, Italy.*
[2] *Camlin Italy Srl, Strada Budellungo 2, 43123 Parma, Italy.*
[3] *Institute for Bioengineering of Catalonia (IBEC), C. Baldiri Reixac, 10-12, 08028 Barcelona, Spain*
[4] *Department of Applied Science and Technology, Politecnico di Torino, C.so Duca degli Abruzzi 24, 10129 Torino, Italy*
[5] *IPCB- CNR, Institute for Polymers, Composites and Biomaterials, P.le E. Fermi, 1, 80055 Portici (Na), Italy.*

[a)]Corresponding author: salvatore.iannotta@imem.cnr.it

Abstract. Organic Electrochemical Transistors (OECTs) represent a versatile tool successfully exploited in the field of Bioelectronics. In particular, OECTs have been used for the detection of a wide set of bioanalytes, often showing superior performance compared to that of commonly used sensors. In this study, we propose a flexible, disposable OECT, based on poly (3,4-ethylenedioxythiophene):polystyrene sulfonate (PEDOT:PSS) channels and few layers graphene (FLG) sheets gate electrodes, for the detection of Tamoxifen (TAM), an important antitumor drug widely used in breast cancer therapy. The optimal device operation conditions in terms of sensitivity and limit of detection (LOD) have been investigated too.

INTRODUCTION

In recent years, devices based on organic semiconductors have gained increasing attention as highly-sensitive bioanalytical tools, due to the ease of processing, the mechanical properties and the marked biocompatibility of organics. In particular, Organic Electro-Chemical Transistors (OECTs) are prototypes of sensing devices showing superior performances in biosensing applications [1]. The noticeable capability of OECTs to implement the detection of bioanalytes is due to their inherent transduction of ionic signals into electronic ones, which allow direct analysis of biological fluids. The working principle of an OECT relies on the reversible modulation of the conductive properties of the transistor channel, made of a highly p-doped conducting polymeric thin film (in most cases, PEDOT:PSS) comprised between a couple of electrodes (source and drain) and in contact with an electrolyte, with an electrode (gate) immersed in. Specifically, the device channel undergoes a reversible electrochemical de-doping (decrease of the source-to-drain channel current, I_{ds}) upon injection of cationic species from the electrolyte into the polymer bulk. The strength of the de-doping process is modulated by the gate electrode, due to a modification of PEDOT:PSS capacitance per unit volume [2]. Fast operating time, miniaturization and low cost, together with sub-voltage operation (<1 V), solution processability of materials and easy integration with microfluidics, represent the hallmarks of OECTs conceived as innovative tools for rapid, sensitive and cost-effective Lab-on-Chip solutions. So far, OECTs have been successfully applied for the detection of a wide class of biomolecules [3,4] and electrically charged systems [5,6]. From the pharmacological point of view, OECTs were also used as Lab on Chip platforms for monitoring the effects induced by drugs on *in vitro* cell cultures [7].

Tamoxifen ([Z]-2-[4-(1, 2-diphenyl-l-butenyl)-phenoxy]-N,N-dimethylethylamine) (TAM) is an oral nonsteroidal antiestrogen widely used in breast cancer therapy and as a chemopreventive agent in healthy women at

NANOINNOVATION 2017
AIP Conf. Proc. 1990, 020015-1–020015-7; https://doi.org/10.1063/1.5047769
Published by AIP Publishing. 978-0-7354-1706-9/$30.00

high risk for developing breast cancer [8]. The detection of residual levels of TAM in plasma of patients treated with this drug (average plasma concentration falling in the range 2-200 ng/ml [9]) allows monitoring the ability of their organism to metabolize the agent and, hence, the degree of advancement of the therapy. However, the detection of TAM levels requires complex experimental techniques such as high-performance liquid chromatography (HPLC) [10,11] rather than non-aqueous capillary electrophoresis (CE) [12]. Thus, in the perspective of easy-to-access tools for point-of-care diagnostics, the development of rapid, portable and low-cost analytical methods for detection of TAM is highly desirable.

In this study, flexible OECTs based on a PEDOT:PSS films and few layer graphene (FLG) sheets (acting as gate electrodes) are used as biosensor for highly sensitive determination of TAM, discussing also the optimal device operation mode in terms of sensitivity and limit of detection (LOD).

MATERIALS AND METHODS

Chemicals were all purchased from Sigma Aldrich. Kapton foils were purchased from DuPont. Eight OECTs based on PEDOT:PSS films (70 nm-thick, deposited by spin coating from a PEDOT:PSS dispersion with 5% and 0.5% in volume of ethylene glycol, EG, and dodecyl benzene sulfonic acid, DBSA, respectively) were fabricated onto a 2 inch Kapton substrate, following a photolithographic method [13]. PEDOT:PSS films were post-baked at 70 °C for 3-5 min. The channel area was 0.6 mm^2 (100 µm x 6 mm, aspect ratio = 60; see the device layout in Fig. 1(a))

Semi-transparent and electrically conductive FLG-coated polymeric films were produced by rubbing out with a low-density-polyethylene (LDPE, surface (20×20 cm, with thickness of ca. 80µm), an alcoholic (ethanol, 99%) suspension of graphene at a concentration of 18g/dm^{-3}. The FLG was prepared according to a method previously reported in literature based on the exfoliation of nanocrystalline graphite [14]. The morphology of FLG-modified LDPE substrates were analysed by atomic force microscopy (AFM). AFM analysis was performed by using a Digital Instruments Nanoscope IIIa (Digital Instruments, Tonawanda, NY, USA) equipped with silicon tips (apical curvature radius of 5 nm). The AFM images were acquired in tapping mode under ambient conditions, with a scan size and rate of 2 µm and 1 Hz, respectively. FLG-modified LDPE films were used as gate electrodes in the form of cylindrical coils, with an exposed area to the electrolyte of about 12 mm^2.

Electrical measurements were performed using a 2-channel source-meter precision unit (Agilent B2902A) controlled by a customized LabView software. Transfer characteristics (I_{ds} *vs.* V_{gs} curves) were recorded by using TAM citrate (MW 563.6, produced by Plantex Ltd. Netanya, Israel) aqueous solutions (0.1M of TAM in methanol, diluted in MilliQ water at different volume ratios in order to get the desired concentration) as the electrolyte and by sweeping the gate bias (V_{gs}) in the range (0,+1.23 V), with a constant drain voltage (V_{ds} = -0.1 V). Different scan rates were used to record I_{ds} *vs.* V_{gs} curves (5, 10, and 30 mV/s, corresponding to a fixed voltage step of 30 mV, and scan times of 6, 3 and 1 s, respectively).

Real-time measurements were performed by initially biasing the sole drain electrode (V_{ds} = -0.1 V) for 30 s in order to let the I_{ds} channel current stabilize, then turning on the gate bias at a fixed value V_{gs} = 0 or V_{gs}=+0.4 V for 200 s. After about 20 s from biasing, 10 µl were removed from the electrolyte (100 µl of MilliQ water) and substituted by injecting a 10µl aliquot containing the appropriate amount of analyte, so that the desired concentration is realized.

RESULTS AND DISCUSSION

The graphene units composing the FLG on LDPE interact each other by π - π physical bonds, and the same type of physical interaction is involved in the adhesion of the FLG-based coating to the polymeric substrate (CH-π bonds).

The special morphology of FLG-coated LDPE films, which are made of different layers, each one consisting of a planar percolative structure, consists of polygonal platelets covering the entire LPDE surface in a continuous and uniform way, as shown by AFM micrographs in Fig. 1(b). Some of the FLG nanocrystals are not completely exfoliated and some crystals adhering to the LDPE substrate are still present, together with some defects produced upon the FLG crystals sliding during the mechanical treatment (Fig. 1(c)).

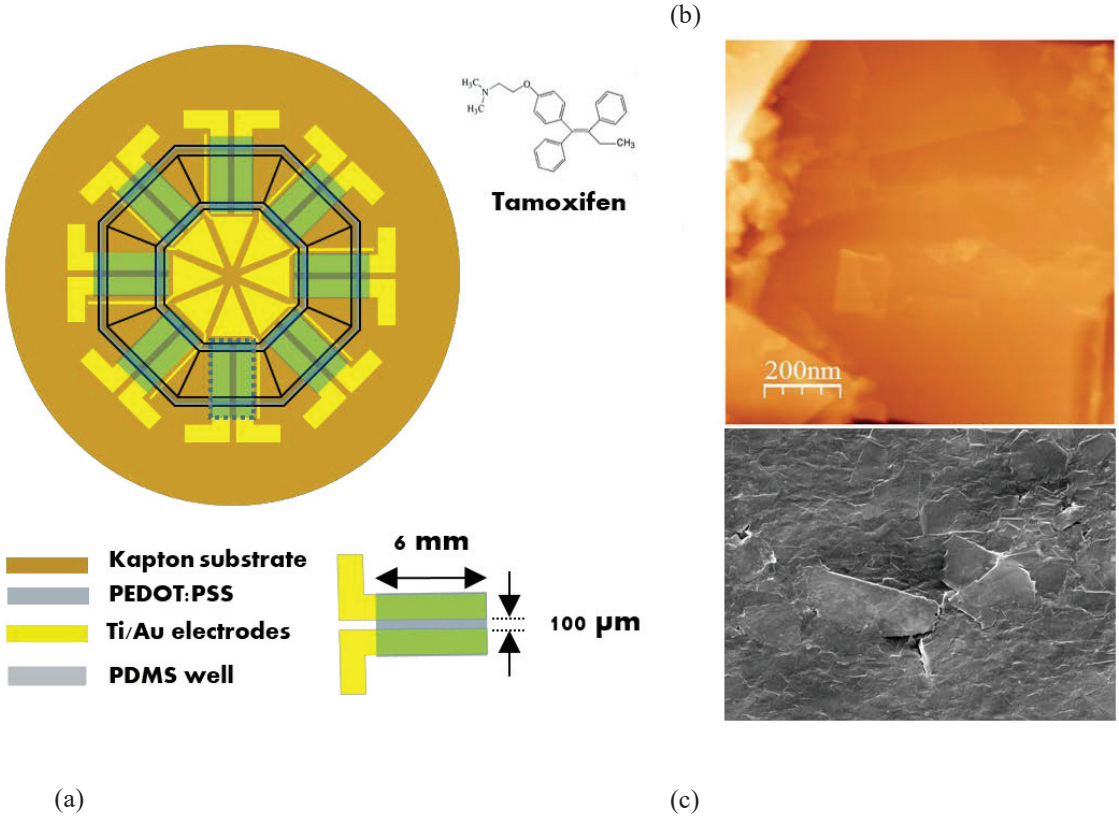

FIGURE 1. (a) OECT layout (inset: molecular structure of TAM); (b) AFM characterization of FLG on LDPE; (c) magnification of an exemplificative defect on the FLG surface by SEM analysis (Reprinted with permission from AIP Conference Proceedings 1599, 18 (2014). Copyright 2014 American Institute of Physics).

The flexile OECT was operated as a sensor of TAM by first measuring its I_{ds} *vs.* V_{gs} curves using the LDPE/FLG sheets as gate electrodes. Figure 2(a) shows the transfer characteristics for increasing concentrations of TAM in MilliQ water (scan rate: 5 mV/s). I_{ds} *vs.* V_{gs} curves show a monotonic decrease of the I_{ds} current upon increasing of the gate voltage. The increase of TAM concentration results in both a slight enhancement of the ON/OFF ratio and a marked shift of the I_{ds} *v.s* V_{gs} curves, towards lower I_{ds} values, at a given V_{gs}. The last observation accounts for an increase of the effective gate voltage (V_{gs}^{eff}) acting on the device channel, due to an offset voltage related to the analyte concentration:

$$V_{gs}^{eff} = V_{gs} + V_{offset} \tag{1}$$

It is possible to merge transfer curves reported in Fig. 2(a) in order to yield a universal curve, as shown in Fig. 2(b), by shifting them horizontally. This shift, providing the dependence of the OECT response on the concentration of TAM, can be expressed as follows:

$$\Delta V_{gs} = V_{offset} = V_{gs}^{eff} - V_{gs} \tag{2}$$

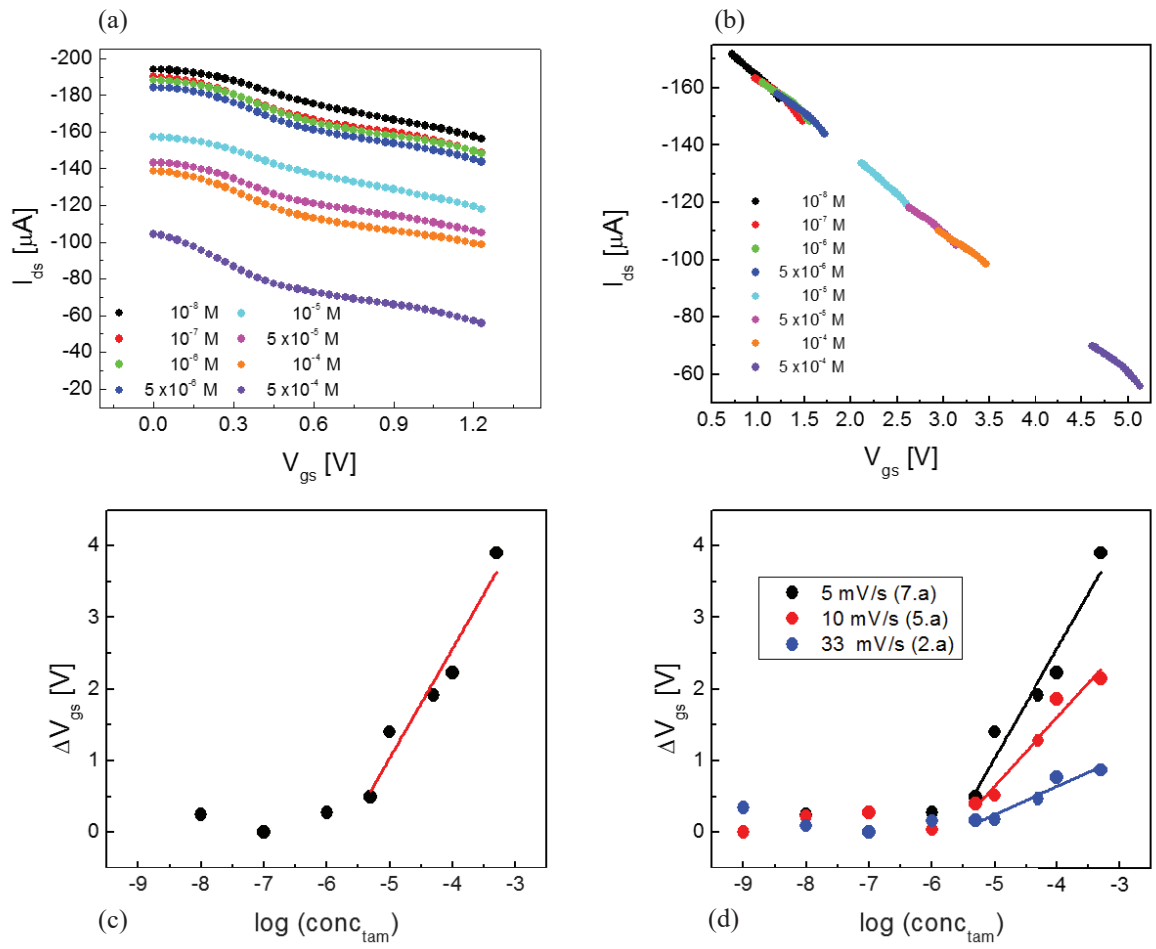

FIGURE 2. (*a*) I_{ds} *vs.* V_{gs} (curves recorded at V_{ds} = -0.1 V, scan rate 5mV/s) for an OECT in presence of TAM at different concentrations in milliQ water. (b) Universal transfer curve obtained by scaling each transfer curve along the x-axis by a factor ΔV_{gs}, related to the concentration of TAM, and (c) related calibration curve. The red line is a linear fit to data in the concentration range 5x10^{-6} – 5x10^{-4} M. (d) Comparison among calibration curves obtained at different scan rates (5, 10 and 30 mV/s).

ΔV_{gs} (reported in Fig. 2(c)) shows a logarithmic dependence on the concentration of TAM up to 5x10^{-4} M. The logarithmic dependence of ΔV_{gs} on the concentration of TAM showed in Fig. 2(c) can be expressed as:

$$\Delta V_{gs} = 2.30(1+\gamma)\frac{KT}{nq}\log(C_{TAM}) + \cos t \qquad \left(\gamma = \frac{C_{ec}}{C_{ge}}\right) \tag{3}$$

where k is Boltzmann's constant, T is temperature, n is the number of electrons transferred at the gate, C_{TAM} is the concentration of TAM, and C_{ec} and C_{ge} are the capacitances at the two gate/electrolyte and electrolyte/PEDOT:PSS interfaces, respectively. Equation 3 implies that the increase of the TAM concentration will increase the effective gate voltage operating in the OECT, thus decreasing the I_{ds} current [6,15].

The device sensitivity, corresponding to the slope of a linear fit to the plot of ΔV_{gs} *vs.* $log(C_{TAM})$ in the dynamic range of the sensor ($5x10^{-6}$ – $5x10^{-4}$ M), was 1530 ± 220 mV/decade, and the LOD was 2.82 µM (equal to1.59 µg/ml). The LOD was estimated as the intersection between the slope of the linear fit and the ideal line passing through the baseline of the ΔV_{gs} data obtained for low TAM concentrations. All transfer curves at a given TAM concentration have shown a variability of the channel current of 1.5% at most.

In order to determine the optimal working condition of the device, transfer curves were also recorded at scan rates of 10 and 30 mV/s (Fig. 2(d)), resulting in sensitivities and LOD of 979 ± 160 mV/decade and 393 ± 60 mV/decade, and 3.12 µM and 5.07 µM, respectively (see Table 1). Therefore, transfer curves measured at the lowest scan rate (5 mV/s) resulted in the highest sensitivity and the lowest LOD.

Table 1. *Sensing parameters obtained from the linear fit of the ΔV_{gs} vs. log (C_{TAM}) plots at different scan rates (5, 10, and 30 mV/s).*

Scan rate [mV/s]	LOD [µM]	Sensitivity [mV/dec]	Linear range [M]	Correlation coefficient [r^2]
5	2.82	1530 ± 220	$5x10^{-6}$ – $5x10^{-4}$	0.92
10	3.12	979 ± 160	$5x10^{-6}$ – $5x10^{-4}$	0.90
33	5.07	393 ± 60	$5x10^{-6}$ – $5x10^{-4}$	0.91

Interestingly, as shown in Fig. 2(a), the I_{ds} values decrease as the concentration of TAM increases even when the gate voltage is set to zero, namely from about 200 µA at 10^{-9} M to about 100 µA at $5x10^{-4}$ M, suggesting that our OECT can effectively operate as a sensor of TAM also at zero gate bias. The I_{ds} lowering at zero gate bias in response to the increase of TAM concentration showed in Fig. 2(a) can be ascribed to the following effects:

- an initial diffusion of ionic species due to hydration properties of channel (TAM molecules are expected to diffuse into PEDOT:PSS through the highly hydrophilic PSS^- phase) [16];
- the capacitive coupling at the device interfaces (that, according to the Gouy-Chapman-Stern theory [17], is sensitive to the TAM concentration);
- the potential gradient generated along the channel by V_{ds} (assisting the drift of some cations towards the bulk of PEDOT:PSS, where the fraction of cations driven by the potential gradient depends on their concentration in the electrolyte).

It is worth to mention that control experiments consisting in baseline curves, i.e. transfer curves measured in the case of pure water as electrolyte, have been carried out in order to ascertain the actual role of tamoxifen as analyte detected by our device.

Real-time measurements have shown to be a useful tool to achieve very low LODs [4]. Such measurements consist in recording changes in the OECT response, at constant V_{ds} and V_{gs}, due to the addition of increasing analyte aliquots to the electrolyte. Figure 3(a) shows the typical I_{ds} *vs. time* curves recorded upon addition of fixed amounts of TAM in MilliQ water and by biasing the gate and drain electrodes at +0.4 V and -0.1 V, respectively. An abrupt decrease of the absolute value of the I_{ds} current, whose magnitude is directly related to the concentration of TAM, is observed upon addition of an aliquot of analyte. The noise level of the I_{ds} current was ~0.06 µA, thus considerably lower than the order of magnitude of the I_{ds} current (~300 µA). The detection limit in real-time mode was found to be 10 nM (equal to 5.63 ng/ml, with a signal-to-noise ratio >3), which is more than two orders of magnitude lower than the LOD obtained from the analysis of transfer characteristics. Control measurements performed by adding aliquots of electrolyte without TAM dissolved in it did not induce any detectable change in the I_{ds} current, thus ruling out the role of the injection as the cause of the changes detected in the I_{ds} current.

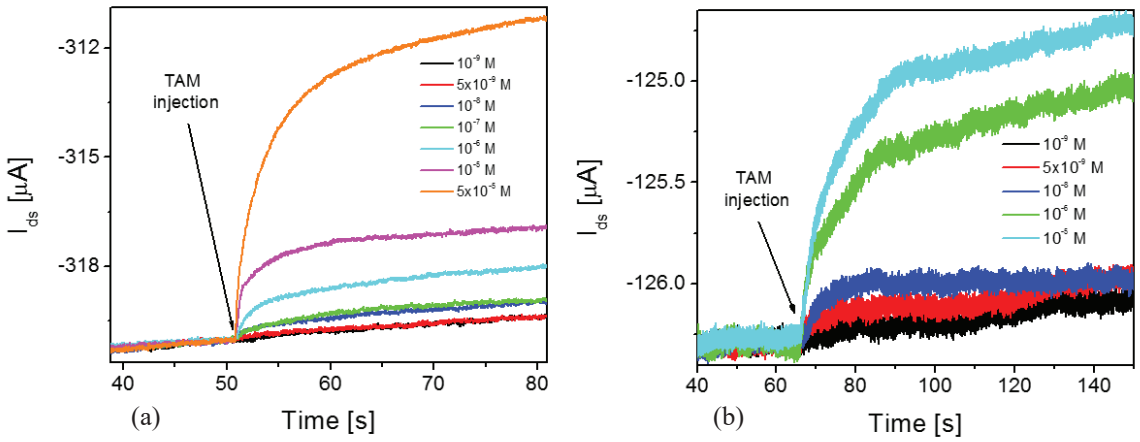

FIGURE 3. I_{ds} vs. time upon injection of aliquots of TAM, where the OECT is operated at V_{ds}= -0.1 V and (a) V_{gs} = 0.4 V (TAM concentration: from 10^{-9}M to $5*10^{-5}$M) or (b) V_{gs} = 0 V (TAM concentration: from 10^{-9}M to 10^{-5}M).

Real-time detection of TAM at V_{gs}=0 was also performed, as reported in Fig. 3(b). In this case, a LOD of 5 nM (equal to 2.82 ng/ml; signal-to-noise ratio = 3) was obtained, which is the lowest LOD achieved in this study. This result suggests that the sensing capability of the device relies on a drifting mechanism of drug molecules into the porous film of PEDOT:PSS.

CONCLUSIONS

OECTs equipped with graphene-based gate electrodes have shown to be a powerful and easy tool for the detection of TAM at concentrations generally accessible to complex and expensive techniques, which are of interest for pharmacologic therapy. The opportune design of the device architecture and the use of real time measurements, suited for measurements in presence of fluid flows, allow defining the optimal detection conditions. In our case, the lowest LOD of 2.82 ng/ml has been assessed for real-time measurements at zero gate bias, being the device able to detect in normal conditions few μg/ml of TAM.

ACKNOWLEDGMENTS

This work has been partially funded by the N-Chem project within the CNR–NANOMAX Flagship program and "THERSEO" project, cofunded by POR-FESR 2014-2020, Regione Emilia Romagna. Authors wish to thank Prof. F. Sonvico, Dept. of Pharmaceutical Chemistry, University of Parma, for providing Tamoxifen.

REFERENCES

1. G. Tarabella, F. Mahvash Mohammadi, N. Coppedè, F. Barbero, S. Iannotta, C. Santato, and F. Cicoira, Chem. Sci. **4**, 1395 (2013).
2. J. Rivnay, P. Leleux, M. Ferro, M. Sessolo, A. Williamson, D. a. Koutsouras, D. Khodagholy, M. Ramuz, X.

Strakosas, R. M. Owens, C. Benar, J.-M. Badier, C. Bernard, and G. G. Malliaras, Sci. Adv. **1**, e1400251 (2015).
3. H. Tang, P. Lin, H. L. W. Chan, and F. Yan, Biosens. Bioelectron. **26**, 4559 (2011).
4. G. Tarabella, A. Pezzella, A. Romeo, P. D'Angelo, N. Coppedè, M. Calicchio, M. D'Ischia, R. Mosca, and S. Iannotta, J. Mater. Chem. B **1**, 3843 (2013).
5. V. Preziosi, G. Tarabella, P. D'Angelo, A. Romeo, M. Barra, S. Guido, A. Cassinese, and S. Iannotta, RSC Adv. **5**, 16554 (2015).
6. M. Sessolo, J. Rivnay, E. Bandiello, G. G. Malliaras, and H. J. Bolink, Adv. Mater. **26**, 4803 (2014).
7. A. Romeo, G. Tarabella, P. D'Angelo, C. Caffarra, D. Cretella, R. Alfieri, P. G. Petronini, and S. Iannotta, Biosens. Bioelectron. (2015).
8. V. C. Jordan, Nat. Rev. Drug Discov. **2**, 205 (2003).
9. A. F. and D. FDA, Http://www.drugs.com/pro/tamoxifen.html (2013).
10. R. R. Brown, R. Bain, and V. C. Jordan, J. Chromatogr. **272**, 351 (1983).
11. K.-H. Lee, B. Ward, Z. Desta, D. Flockhart, and D. R. Jones, J. Chromatogr. B. Analyt. Technol. Biomed. Life Sci. **791**, 245 (2003).
12. J. R. Flores, J. J. B. Nevado, A. M. C. Salcedo, and M. P. C. Díaz, Talanta **65**, 155 (2005).
13. S. Ouyang, Y. Xie, D. Zhu, X. Xu, D. Wang, T. Tan, and H. H. Fong, Org. Electron. **15**, 1822 (2014).
14. G. Carotenuto, S. De Nicola, G. Ausanio, D. Massarotti, L. Nicolais, and G. P. Pepe, Nanoscale Res. Lett. **9**, 475 (2014).
15. P. Lin, F. Yan, and H. L. W. Chan, Appl. Mater. Interfaces **2**, 1637 (2010).
16. P. D'Angelo, N. Coppedè, G. Tarabella, A. Romeo, F. Gentile, S. Iannotta, E. Di Fabrizio, and R. Mosca, Org. Electron. **15**, 3016 (2014).
17. A. J. Bard and L. R. Faulkner, *Electrochemical Methods: Fundamentals and Applications, 2nd Edition* (John Wiley & Sons, Inc., New York, 2001).